Contribution from the Research Laboratories,
Eastman Kodak Company, Rochester, New York 14650

Kinetics and Mechanism of Chelation of Nickel(II) by 2-(2-Pyridylazo)-1-naphthol (α-PAN) Dyes

RICHARD L. REEVES,* GARY S. CALABRESE, and SHELLEY A. HARKAWAY

Received December 29, 1982

The chelation kinetics and equilibria with two α-PAN dyes were studied in several amine buffers and in noncomplexing zwitterionic buffers in the pH range of 4–10.3 at nickel concentrations where the 1:1 complex, MD, is the predominant or exclusive product at equilibrium. In a 10- to 20-fold excess of nickel, the rapid chelation gives a kinetically controlled mixture of MD and the 1:2 complex, MD_2, in which the concentration of MD_2 exceeds its equilibrium level. Equilibration of MD_2 to MD had half-times of several hours. The excess MD_2 forms from MD and unreacted dye in consecutive, parallel reactions whereby $k_{MD_2} \simeq 5k_{MD}$. At pH 8 and $[Ni]_T < 0.4$ mM the rate-determining step (rds) is the initial substitution to form a unidentate intermediate. At high $[Ni]_T$ (0.1 M) the rds changes to ring closure. At $[Ni]_T$ near 0.01 M initial ligation and ring closure proceed at comparable rates, and rate constants for both steps are estimated. Kinetic and spectral arguments suggest that the final ring closure from the bidentate intermediate is abnormally slow ($k_3 \simeq 25\ s^{-1}$). Kinetic analysis indicates that both the uni- and bidentate intermediates partition in the forward and reverse directions with partition coefficients near unity. It is suggested that the large value of k_{MD_2} and a large catalytic effect of imidazole compared to those of nonaromatic amines of similar basicity and ligand strength result from an enhanced value of the outer-sphere complex constant whereby prior complexation by the aromatic ligand facilitates entry of dye through a stacking interaction.

Introduction

Several studies of the kinetics of chelation of nickel(II) by pyridylazo ligands have appeared. These involved the bidentate ligand 4-(2-pyridylazo)dimethylaniline (PADA)[1-5] and the tridentate ligands 4-(2-pyridylazo)resorcinol (PAR)[6,7] and 1-(2-pyridylazo)-2-naphthol (β-PAN).[8,9] The stoichiometries of these complexes vary among the dyes. In an excess of nickel, PADA forms a 1:1 nickel–dye complex, where the rate-determining step (rds) is loss of the first water from the inner coordination sphere. Chelation of nickel(II) by β-PAN is reported to give the 1:1 complex with a large excess of nickel[8] and the 1:2 complex with a moderate excess.[9] Chelation of nickel(II) and cobalt(II) by PAR is reported to give the 1:2 complexes with an excess of metal ion.[10] Widely disparate values of the stability constants for the nickel–PAR complexes have been published.[11,12] With either set of values for these and those for the cobalt(II)–PAR complexes,[11] a calculation shows that the 1:1 complex should be the predominant or exclusive product formed under thermodynamic control with an excess of the metal ion. This suggested that kinetically controlled products might form from the rapid chelation in some of these systems. We show here that this can be the case.

The large difference in reactivity between PAR and β-PAN with nickel(II) and cobalt(II) also raises questions. The value of the forward rate constant k_f for the chelation of nickel(II) by PAR is close to that expected if loss of the first water from the coordination shell is the rds.[6] Since the 1:2 complex is the product, the rate constant for adding a second molecule of PAR must be larger than that for adding the first, and this raises the possibility that stacking interactions between the dyes may be important in forming the bis complex.[13] Azo dyes of this type do have a strong tendency to stack.[14] In contrast, k_f for forming the 1:1 Ni–β-PAN complex with a large excess of nickel is less by several orders than that expected if initial ligation is the rds. The interpretation was that, with β-PAN, the rds was the final ring closure, which involves the breaking of the internal hydrogen bond between the ortho hydroxyl and an azo nitrogen, followed by rotation of the naphthol group.[8] PAR and β-PAN both have stable hydrogen-bonded hydroxyl groups, however, as judged by their similar high pK_a's for dissociation of this proton,[15] so the role of the hydrogen bond in the kinetics is not clear.

We report here a kinetic study of the chelation of nickel(II) by two solubilized 2-(2-pyridylazo)-1-naphthol (α-PAN) dyes (I and II) in a variety of complexing (amine) and noncomplexing (zwitterionic) buffers. To our knowledge, studies of such ligands have not been reported previously. The chelation kinetics are more complex than those reported for other pyridylazo ligands, but in understanding the complexities we have gained new insights into the chelation mechanism. We show that the initial product mixture is formed by kinetic control whereby the bis complex forms from the 1:1 complex by an unusually fast reaction. We also show that initial bond formation is rate determining at low nickel concentrations, but ring closure becomes rate limiting at high nickel concentrations. Rate constants for formation and decay of the intermediate are estimated at intermediate nickel concentrations.

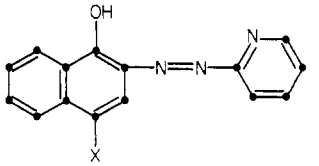

I, X = SO_3H
II, X = $SO_2N(C_2H_4OSO_3NH_4^+)_2$

Experimental Section

Materials. The dyes were synthesized in house or were gifts. Minor colored impurities were removed from dye I by preparative-scale chromatography on Sephadex G-25.[16] The dye sulfonic acid was

(1) Wilkins, R. G. *Inorg. Chem.* **1964**, *3*, 520.
(2) Cobb, M. A.; Hague, D. N. *J. Chem. Soc., Faraday Trans. 1* **1972**, *68*, 932.
(3) Bennetto, H. P.; Imani, Z. S. *J. Chem. Soc., Faraday Trans. 1* **1975**, *71*, 1143.
(4) James, A. D.; Robinson, B. H. *J. Chem. Soc., Faraday Trans. 1* **1978**, *74*, 10.
(5) Robinson, B. H.; White, N. C. *J. Chem. Soc., Faraday Trans. 1* **1978**, *74*, 2625.
(6) Funahashi, S.; Tanaka, M. *Inorg. Chem.* **1969**, *8*, 2159.
(7) Holyer, R. H.; Hubbard, C. D.; Kettle, S. F. A.; Wilkins, R. G. *Inorg. Chem.* **1966**, *5*, 622.
(8) Hubbard, C. D.; Pacheco, D. *J. Inorg. Nucl. Chem.* **1977**, *39*, 1373.
(9) Mochizuki, K.; Imamura, T.; Ito, T.; Fujimoto, M. *Chem. Lett.* **1977**, 1239.
(10) Mochizuki, K.; Imamura, T.; Ito, T.; Fujimoto, M. *Bull. Chem. Soc. Jpn.* **1978**, *51*, 1743.
(11) Geary, W. J.; Nickless, G.; Pollard, F. H. *Anal. Chim. Acta* **1962**, *27*, 71.
(12) Corsini, A.; Fernando, Q.; Freiser, H. *Inorg. Chem.* **1963**, *2*, 224.
(13) Margerum, D. W.; Cayley, G. R.; Weatherburn, D. C.; Pagenkopf, G. K. In "Coordination Chemistry, Vol. 2"; Martell, A. E., Ed.; American Chemical Society: Washington, DC, 1978; ACS Monogr. No. 174, p 140.
(14) Reeves, R. L.; Maggio, M. S.; Harkaway, S. A. *J. Phys. Chem.* **1979**, *83*, 2359 and references cited therein.
(15) Sillen, L. G.; Martell, A. E. *Spec. Publ.—Chem. Soc.* **1964**, *No. 17*.
(16) Reeves, R. L.; Kaiser, R. S.; Finley, K. T. *J. Chromatogr.* **1970**, *47*, 217.

0020-1669/83/1322-3076$01.50/0 © 1983 American Chemical Society

isolated from the acidified eluate. Atomic absorption, thermal gravimetric, and elemental analyses confirmed the absence of sodium and water. The sample of dye II gave a satisfactory elemental analysis and was used as received.

The buffers were recrystallized twice from a mixture of deionized water and ethanol that had been distilled in an all-glass still. Imidazole and 2-methylimidazole were recrystallized from ethyl acetate/isooctane. A small amount of EDTA or 2,2′-bipyridine was added in the first recrystallization to remove any trace metals in the samples. CHES was Fluka puriss. grade and was used as received. An aqueous stock solution of perchloric acid was prepared from Alfa Products Ultrapure 70% perchloric acid. Stock solutions of nickel perchlorate were prepared by dissolving the stoichiometric amount of Johnson Matthey Chemicals, Ltd. "Puratronic" basic nickel carbonate in the perchloric acid stock solution and adjusting the pH to 5.5. The solution was standardized with EDTA solution with pyrocatechol violet as the end-point indicator.

Kinetic Measurements. Rapid measurements were made at 25 °C on the Durrum stopped-flow spectrophotometer. Precipitation of nickel hydroxide at high pH before reaction was avoided by mixing a nickel solution in deionized water with the dye in buffer. Up to pH 11 the chelation was complete before nickel hydroxide precipitated. When the nickel salt was placed in noncomplexing buffers first, light scattering could be seen at pH above 7.5. Digital coordinates (transmittance vs. time) were read from the oscilloscope traces with a Tektronix Model 4662 interactive plotter. Transmittance values were converted to absorbance via a Tektronix Model 4051 microcomputer and were fitted to a linear first-order function ($\ln (A - A_\infty)$ vs. time) by linear regression. In addition to the rate constant and the correlation coefficient, the program printed out the residuals (differences between the observed values of $\ln (A - A_\infty)$ and those computed by regression). When the reactions actually followed first-order kinetics, data collected through 85–90% reaction gave correlation coefficients of 0.9997–1.000 with random residuals. Fits with correlation coefficients of 0.9995 or less usually gave a pattern of residuals that indicated that the observed data were giving curved first-order plots. In these cases, data were eliminated from the end of the reaction until linear regression on the retained data points gave random residuals.

The rapid biphasic kinetic data obtained at high nickel concentrations were fitted to eq 13 by nonlinear regression in both the exponential and logarithmic forms. Although the same parameter values were obtained within experimental error by either model, we found that the logarithmic form provided greater sensitivity in estimating the parameters in the second term of eq 13.

The very slow phase of the overall biphasic reaction was measured on a Cary 118C spectrophotometer with a 10-fold excess of nickel. For the slow reactions, equal volumes of the dye and nickel solutions were mixed from motor-driven syringes through a mixing "tee". The precision for replicate mixings was 0.42%. The rapid phase of the reaction had proceeded to completion by the time the first absorption curve was measured. Rates of conversion of authentic 1:2 complex to the 1:1 complex with excess nickel(II) were measured in separate experiments by first forming the 1:2 complex in situ by equilibrating nickel and dye at a stoichiometric ratio of 0.5 for 18 h. The rate measurement was initiated by adding a 10-fold excess of nickel to the preformed complex.

Product Yields. The relative amounts of the two complexes formed at the end of the rapid phase of the chelation were measured spectrophotometrically as the fractional difference between the absorbance at 516 nm and the absorbance difference of the pure complexes at the same wavelength. The latter absorbances were obtained by equilibrating solutions for 18 h at stoichiometric ratios of 50 and 0.5, respectively.

Results

The buffers, their acronyms, their pK_a's, and the stability constants for amine complexes with nickel(II) are given in Table I. Good et al. have reported that a number of zwitterionic buffers such as those used here, including MES, give undetectable complexation with copper(II).[17] The fact that rate constants obtained in HEPPS are the same as those obtained by extrapolation to zero Tris buffer concentration shows that complexation of HEPPS with nickel(II) is negligible. Evidence that CHES is also noncomplexing is the fact that rate constants in CHES and HEPPS are the same in overlapping pH ranges.

Table I. Physical Constants of Buffers at 25 °C

buffer	pK_a	formation constants: log K_1	log K_2	log K_3
imidazole (Im)	7.103[a]	3.09[b]	2.47	2.00
2-methylimidazole (2-MeIm)	7.851[c]			
$H_2NC(CH_2OH)_3$ (Tris)	8.074[d]	2.63[e]	1.9	
$N(CH_2CH_2OH)_3$ (TEA)	7.762[f]	3.43[g]	2.20	1.37
morpholinoethanesulfonic acid (MES)	6.1			
N-(2-hydroxyethyl)piperazine-*N*′-3-propanesulfonic acid (HEPPS)	7.9			
2-(cyclohexylamino)ethanesulfonic acid (CHES)	9.3			

[a] Datta, S. P.; Grzybowski, A. K. *J. Chem. Soc.* **1966**, 1059. [b] Sklenskaya, E. V.; Karapet'yants, M. Kh. *Zh. Neorg. Khim.* **1966**, *11*, 2061; *Russ. J. Inorg. Chem. (Engl. Transl.)* **1966**, *11*, 1102. [c] Kirby, A. H. M.; Neuberger, A. *Biochem. J.* **1938**, *32*, 1146. [d] Bates, R. G.; Hetzer, H. B. *J. Phys. Chem.* **1961**, *65*, 667. [e] Bai, K. S.; Martell, A. E. *J. Inorg. Nucl. Chem.* **1969**, *31*, 1697. [f] Bates, R. G.; Allen, G. F. *J. Res. Natl. Bur. Stand., Sect. A* **1960**, *64A*, 343. [g] Sklenskaya, E. V.; Karapet'yants, M. Kh. *Zh. Neorg. Khim.* **1966**, *11*, 2749; *Russ. J. Inorg. Chem. (Engl. Transl.)* **1966**, *11*, 1478.

When dilute, dust-free solutions of the dyes and nickel(II) were allowed to stand overnight in water or in the zwitterionic buffers, slow spectral changes with diffuse isosbestic points occurred and there was an increase in scattered light. Slow spectral changes also occurred in the amine buffers, but the solutions remained homogeneous for 24 h and isosbestic points were sharp. The amine buffers were used to study the slow equilibration, whereas the noncomplexing zwitterionic buffers were used to study the rapid chelation kinetics.

Equilibria and Spectra. The pK_{a2} values for ionization of the naphthol OH groups in I and II were determined spectrophotometrically to be 8.14 and 7.43, respectively.

Figure 1 shows the absorption curves of dye II at pH 8.2 and the 1:1 and 1:2 complexes in Tris buffer. The two complexes have the same absorptivity at 460 nm, the dye and the 1:1 complex (MD)[18] have the same absorptivity at 492 nm, and the dye and the 1:2 complex (MD_2) have the same absorptivity at 497 nm. At pH 8.2 the dye is 85% dissociated. Similar curves were obtained for dye I. Successive additions of nickel(II) to a constant concentration of dye and equilibration for 18 h gave two distinct spectral changes. Absorption curves measured at stoichiometric Ni:dye ratios (R) up to 0.5 had a clean isosbestic point. The spectral change corresponds to the conversion of dye to MD_2. A second change with a new isosbestic point occurs at $0.5 < R < 20$, corresponding to the conversion of MD_2 to MD. The same results were obtained from spectral titrations made over a range of pH 4.8–9. Calculation of equilibrium concentrations of the various species from the stability constants (see below) confirmed that the measured curve at $R = 0.5$ was that of pure MD_2.

The spectral changes were used to measure the ratio of the successive formation constants of the two complexes. The formation constants were defined in the usual way by eq 1 and 2 where D represents fully dissociated dye and M is Ni-

$$M + D \rightleftarrows MD \quad K_{1f} \tag{1}$$

$$MD + D \rightleftarrows MD_2 \quad K_{2f} \tag{2}$$

(17) Good, N. E.; Winget, G. D.; Winter, W.; Connolly, T. N.; Izawa, S.; Singh, R. M. M. *Biochemistry* **1966**, *5*, 467.

(18) Throughout this paper we let MD and MD_2 represent stoichiometric complexes of nickel with the tridentate dyes and reserve the conventional symbol L for individual ligand groups within the dye.

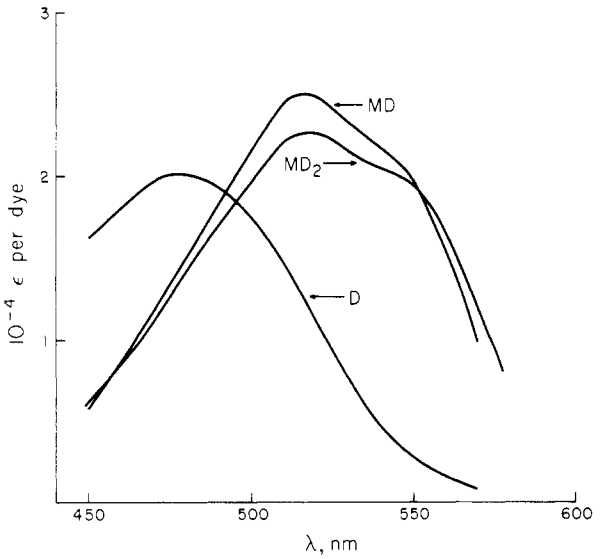

Figure 1. Absorption curves of dye II and of the 1:1 and 1:2 Ni–dye complexes in pH 8.2 Tris buffer. The curve of MD_2 was measured at a stoichiometric Ni:dye ratio of 0.5 and that of MD at a ratio of 20. The absorptivities per mole of dye duplicate the curves and isosbestic points observed when various amounts of nickel(II) are added to a constant concentration of dye. If absorptivities were given in terms of moles of complex, the amplitude of the curve for MD_2 would be twice that shown.

$(H_2O)_6^{2+}$. The apparent "titrimetric" equilibria corresponding to the two spectral changes are defined by

$$M + 2D \rightleftarrows MD_2 \qquad K_1 \equiv \frac{[MD_2]}{[M][D]^2} = K_{1f}K_{2f} \qquad (3)$$

for $0 < R < 0.5$ and

$$MD_2 + M \rightleftarrows 2MD \qquad K_2 \equiv \frac{[MD]^2}{[MD_2][M]} = \frac{K_{1f}}{K_{2f}} \qquad (4)$$

for $0.5 < R < 20$. K_1 is thus a very large number, which explains why conversion of dye to the 1:2 complex is quantitative at $R < 0.5$. The spectral titrations show that MD_2 is quantitatively converted to MD only with excess Ni(II), so that K_2 is not large and can be measured directly from the spectral titration. In the region of the titration where $R > 0.5$, no uncomplexed dye is present and

$$[MD] = [D]_T - 2[MD_2] \qquad (5)$$

$$[M] = [M]_T - [MD] - [MD_2] = [M]_T - [D]_T + [MD_2] \qquad (6)$$

where the subscripts represent the stoichiometric concentrations. We let α equal the fraction of the dye present as MD

$$\alpha = \frac{[MD]}{[D]_T} = \frac{A - A_{MD_2}}{A_{MD} - A_{MD_2}}$$

where A_{MD}, A_{MD_2}, and A are the absorbances at an appropriate wavelength of pure MD, pure MD_2, and a mixture, respectively. The fraction of MD_2 is $(1 - \alpha)/2$. Appropriate substitution into eq 4 gives

$$K_2 = \frac{(\alpha[D]_T)^2}{((1 - \alpha)/2)[D]_T([M]_T - [D]_T + [MD_2])} \qquad (7)$$

Dividing by $[D]_T^2$ and collecting terms give

$$K_2 = \frac{\alpha^2}{((1 - \alpha)/2)(R - 0.5 - \alpha/2)} \qquad (8)$$

where $R = [M]_T/[D]_T$.

Absorption curves were measured at a series of R values between 0.5 and 20 in a pH 4.76 acetate buffer at an acetate concentration where complexing with Ni(II) is negligible. Values of K_2 computed via eq 8 were invariant within experimental error over a range of α values. The mean value for dye II was 3.6 with a standard deviation of 0.6. The results show that the formation constants for the 1:1 and 1:2 complexes are nearly the same, in agreement with values reported for β-PAN.[19] Because the values are similar, the individual constants cannot be evaluated from the spectral titrations. Using the experimentally determined ratio of the stability constants and reasonable values of about 10^{12} for the constants,[19] we computed concentrations of the three dye species for various R values by simultaneous solution of eq 1 and 2, the ionization equation for the OH group (K_{a2}), and the material-balance equations.

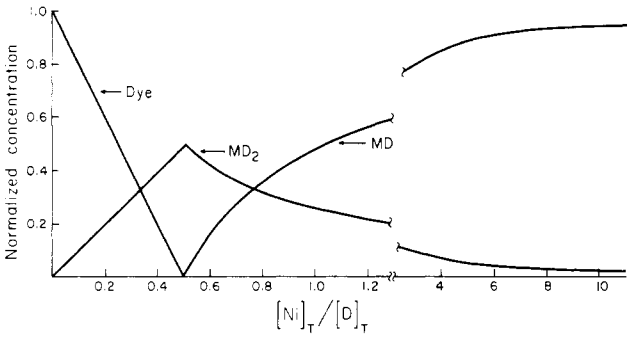

Figure 2. Calculated concentration profiles for the three species of dye II as a function of the Ni:dye ratio at pH 8.2. The calculation was done by using $[dye]_T = 2 \times 10^5$ M. $K_{1f}/K_{2f} = 3.6$ (experimental value), and $K_{1f} = 10^{12}$ (estimated). Normalized concentrations were obtained by dividing the calculated concentrations by the total dye concentration.

Typical concentration profiles for the species of dye II are shown in Figure 2. Identical profiles were obtained for other assumed values of K_{1f} and K_{2f} in the range 10^9–10^{14} M^{-1}, so long as the ratio of the constants was fixed at the experimental value. The simulations show that when $K_{1f}/K_{2f} = 3.6$, quantitative conversion of dye to MD_2 is expected in the range $0 < R < 0.5$ for a wide range of assumed values of the individual formation constants, as found experimentally. They also show that, with a 10-fold excess of nickel(II) and a stoichiometric dye concentration of 2×10^{-5} M, 94% of the dye should be present as MD at equilibrium and conversion to MD should be quantitative with a 20-fold excess.

Overall Kinetics. Runs made with a 10- to 20-fold excess of nickel(II) showed biphasic kinetics. The initial rapid stage had half-times of less than 1 s and depended upon pH, nickel concentration, ionic strength, amine buffer concentration, and the nature of the amine buffer. The second stage had half-times of several hours and was nearly independent of concentration variations. The large difference in the rates of the two phases permitted them to be studied independently.

Absorption curves measured when the initial fast reaction was complete at pH 6.2 (MES), 7.9 (HEPPS), and 8.9 (Tris) showed the presence of a mixture of the 1:1 and 1:2 complexes. With a moderate excess of nickel, the concentration of the 1:2 complex was invariably higher than at equilibrium. Table II compares the fraction of the initial dye present as the 1:1 complex after the initial rapid phase in Tris buffer with that present at equilibrium as a function of the excess nickel concentration. The ratio of the two complexes present at the end of the initial burst varies with the amount of excess nickel.

Spectral and kinetic evidence showed that the slow phase of the biphasic reaction with a 10-fold excess of Ni(II) involved

(19) Corsini, A.; Yih, I.; Fernando, Q.; Freiser, H. *Anal. Chem.* **1962**, *34*, 1090.

Table II. Fraction of Dye Appearing as the 1:1 Complex after the Rapid Chelation and at Equilibrium in pH 8.2 Tris Buffer

Ni:dye[a]	initial	equilibrium
	Dye I	
10	0.70	0.92
20	0.80	0.97
50	0.83	1.0
100	0.88	1.0
	Dye II	
10	0.64	0.96 (0.945 calcd)
20	0.79	1.0
50	0.90	1.0

[a] Dye concentration 2.0×10^{-5} M.

the conversion of the excess MD_2 to its equilibrium level, i.e., the conversion of MD_2 to MD. The time-dependent absorption curves measured throughout the slow phase were identical with curves from equilibrated solutions containing mixtures of MD and MD_2 ($0.5 < R < 20$, Figure 2). Difference spectra of the equilibrated solutions and the time-dependent spectra for the slow phase confirmed that the isosbestic points were identical.

The rate of the slow phase of the biphasic reaction with a 10-fold excess of Ni(II) was the same as the rate of conversion of authentic MD_2 to MD under the same conditions. The latter rate was measured by equilibrating Ni(II) and dye at $R = 0.5$ (Figure 2) and then adding the excess Ni(II). The pseudo-first-order rate constant for the second phase of the biphasic reaction of dye I with a 10-fold excess of Ni(II) was 5.6×10^{-4} s^{-1} in a pH 7.4 imidazole buffer ([Im] = 0.01 M, $\mu = 0.04$). The corresponding rate constant for formation of MD from authentic MD_2 under the same conditions was 5.3×10^{-4} s^{-1}. Similar values for the two rate constants were obtained at other pH values and in other buffers.

The presence of the 1:2 complex in the product mixture formed during the initial burst was further confirmed by comparison of the rates of demetalization with excess ethylenedinitrilotetraacetic acid (EDTA). The 1:1 complex is destroyed rapidly by EDTA, whereas the 1:2 complex reacts slowly. In one experiment, dye was rapidly mixed with a 10-fold excess of Ni(II) to give the initial mixture of products and a large excess of EDTA was then added immediately. The slow rate of uncomplexing was followed spectrophotometrically. In a separate experiment, MD_2 was formed in situ by equilibration of Ni(II) and dye ($R = 0.5$) and then an excess of EDTA was added. The pseudo-first-order rate constants for the two experiments with dye I run in a pH 7.4 imidazole buffer were 1.4×10^{-4} and 1.5×10^{-4} s^{-1}, respectively. We have no explanation at this time for why the slow rate of conversion of MD_2 to MD in excess nickel is faster than the rate of dissociation of MD_2 in excess EDTA. The rate of conversion of MD_2 to MD was independent of pH, ionic strength, and Ni(II) concentration but depended upon the nature of the amine buffer. This suggests that the rate-limiting process in the conversion of MD_2 is not a simple unimolecular dissociation.

Kinetics of the Rapid Phase. All results cited hereinafter will refer to stopped-flow measurements of the rapid initial chelation reaction. The fitting of data taken at different wavelengths to a first-order rate expression usually showed curvature with a 10- to 20-fold excess of nickel ion, with the direction and extent of curvature depending upon the wavelength. Such behavior is expected from a reaction sequence whereby the 1:2 complex forms from the 1:1 complex by a competitive, consecutive mechanism:

$$M + D \xrightarrow{k_{MD}} MD \quad (9)$$

$$MD + D \xrightarrow{k_{MD_2}} MD_2 \quad (10)$$

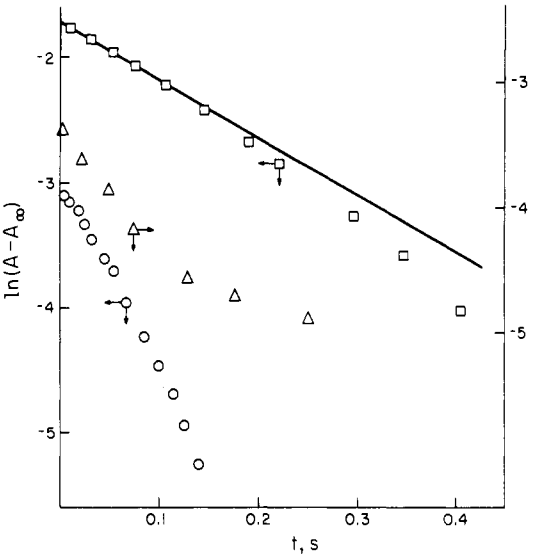

Figure 3. Rates of chelation of nickel(II) by dye II measured at different wavelengths and plotted as a pseudo-first-order reaction: squares, dye disappearance at 460 nm in pH 8.2 HEPPS; triangles, appearance of the 1:1 complex at 497 nm in pH 8.2 Tris; circles, appearance of the 1:2 complex at 492 nm in pH 8.2 Tris.

The rate equation for this sequence with a constant excess of nickel is

$$-\mathrm{d} \ln [D]/\mathrm{d}t = k_{MD}' + k_{MD_2}[MD] \neq \text{constant} \quad (11)$$

where

$$k_{MD}' = k_{MD}[M]$$

The rate law predicts that a first-order plot of absorbance data that measure only the disappearance of dye will have increasing slope as the reaction progresses. Similarly, such a plot for data that measure only the formation of MD and MD_2 will have decreasing and increasing slopes, respectively, as reaction proceeds. First-order plots of data for dye II taken at 460 nm (dye disappearance, Figure 1), 492 nm (formation of MD_2), and 497 nm (formation of MD) are shown in Figure 3 and confirm the predictions of reactions 9 and 10.

In the results to follow we cite rate constants obtained from the initial slopes of first-order plots, k_{init}. These values are close approximations to k_{MD}'.

The sequence given in reactions 9 and 10 accounts for the decreasing initial yield of kinetically controlled 1:2 complex with increasing nickel concentration, since the rate of reaction 9 depends upon the nickel concentration whereas that of reaction 10 does not. Curvature of first-order plots diminished also as the excess of nickel was increased, owing to the reduced formation of MD_2. The scheme given by eq 9 and 10 was modeled by computer to determine the relative values of k_{MD} and k_{MD_2} that would be required to give the experimental product ratio with a 10-fold excess of nickel. With initial concentrations fixed at the experimental values of 2×10^{-5} and 2×10^{-4} M for dye and nickel and k_{MD} fixed at 7.0×10^4 M^{-1} s^{-1} (see below), 35% of the dye would go to MD_2 when the value of k_{MD_2} was 5 times the value of k_{MD}.

Figure 4 shows a qualitative representation of the free energy relationships in forming MD_2 via MD for dye II. The ground-state $\Delta G°$'s are to scale, but the activation barriers are qualitative and merely show that $\Delta G_2^* < \Delta G_1^*$. The MD_2 formed by the kinetically controlled process is converted to MD in the presence of excess metal ion by equilibrium 4, where the initial and final states for dye II differ by only 0.8 kcal mol^{-1} but where a high activation barrier must be passed.

Effect of Nickel Concentration. The initial pseudo-first-order rate constants show a linear dependence on the nickel

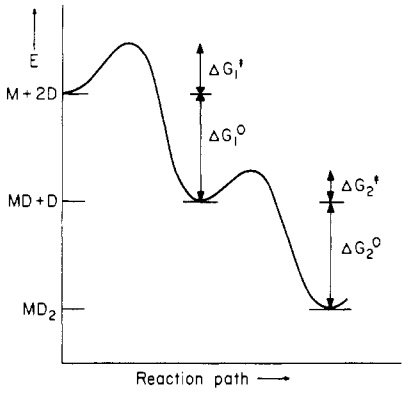

Figure 4. Free energy relationships for forming MD_2 via MD.

concentration in a pH 8.2 HEPPS buffer containing a 10- to 40-fold excess of nickel(II) (0.1–0.4 nM). The values of k_{MD} obtained from the slopes of plots of k_{init} vs. $[Ni^{2+}]$ are 1.6×10^4 and 3.7×10^4 M^{-1} s^{-1} for I and II, respectively. Corresponding values obtained at the same pH in Tris buffer are 3.7×10^4 and 7.0×10^4 M^{-1} s^{-1}. As is shown below, these values are not "pure" rate constants for specific species. At higher nickel concentrations, deviations from linearity were found. Individual first-order plots began to display upward curvature at nickel concentrations greater than 5 mM. At concentrations near 10 mM, it was evident that the rapid chelation was proceeding by two first-order relaxations (Figure 5). The rate of the first relaxation was dependent upon the nickel concentration whereas that of the second was not. This kinetic behavior suggested that an intermediate was accumulating during the chelation according to eq 12. At a given

$$M + D \underset{k_{-a}}{\overset{k_a}{\rightleftharpoons}} X \xrightarrow{k_b} MD \qquad (12)$$

excess of nickel(II), $k_a[M]_T = k_a'$ and the forward and reverse steps all become first-order and the rate equations can be solved in closed form. The solutions are[20]

$$[D] = C_1 e^{-(w+v)t} + C_2 e^{-(w-v)t} \qquad (13)$$

$$\frac{[X]}{[D]_0} = \frac{k_a'(e^{m_1 t} - e^{m_2 t})}{m_1 - m_2} \qquad (14)$$

where

$$m_1 = [-(k_a' + k_{-a} + k_b) + [(k_a' + k_{-a} + k_b)^2 - 4k_a'k_b]^{1/2}]/2$$

and

$$m_2 = [-(k_a' + k_{-a} + k_b) - [(k_a' + k_{-a} + k_b)^2 - 4k_a'k_b]^{1/2}]/2$$

With the assumption that the measured absorbance changes were proportional to $[D] = f(t)$, eq 13 was used to obtain the continuous curves drawn through the data points in Figure 5. The functions of the rate constants in eq 12 were computed from eq 15–17 by use of the best estimates of the fitting constants.

$$k_{-a} + k_b = w - [(C_1 - C_2)/(C_1 + C_2)]v \qquad (15)$$

$$k_a' = w + [(C_1 - C_2)/(C_1 + C_2)]v \qquad (16)$$

$$1 + k_b/k_{-a} = \frac{w^2 - [(C_1 - C_2)/(C_1 + C_2)]^2 v^2}{v^2[1 - [(C_1 - C_2)/(C_1 + C_2)]^2]} \qquad (17)$$

(20) Reeves, R. L.; Tong, L. K. J. *J. Am. Chem. Soc.* **1962**, *84*, 2050.

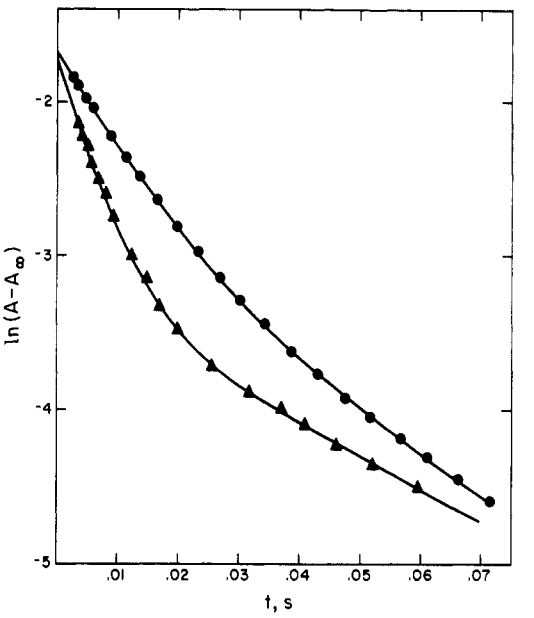

Figure 5. Biphasic kinetics for chelation by dye I resulting from the accumulation of an intermediate at moderately high nickel concentrations: circles, 0.006 M Ni; triangles, 0.014 M Ni. The continuous curves were calculated by fitting the data by eq 13.

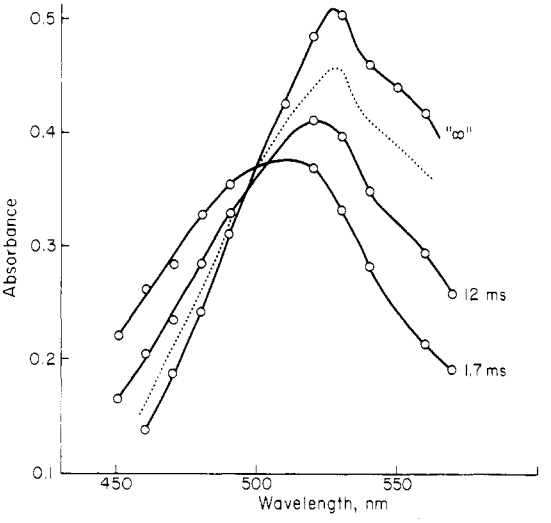

Figure 6. Constructed absorption curves as a function of reaction time for the chelation of Ni^{2+} by dye I under conditions where the intermediate accumulates. Buffer is pH 8.2 HEPPS; $[Ni^{2+}] = 0.008$ M; [dye] = 1.0×10^{-5} M. Data points are omitted for clarity at wavelengths near where the curves cross. The dashed curve is that of a solution containing about 90% intermediate, measured in 0.1 M $NiSO_4$.

To confirm that the kinetic behavior shown in Figure 5 was actually the result of the accumulation of an intermediate, runs were made at multiple wavelengths at a fixed nickel concentration so that absorption curves could be constructed as a function of reaction time. The results are shown in Figure 6. The times shown are the elapsed times following cessation of flow and are not corrected for instrument dead time. If significant concentrations of an intermediate were present during the reaction, an isosbestic point would not be expected. The constructed curves in Figure 6 show the absence of an isosbestic point. The absence of such a point was confirmed by recording oscilloscope traces at high sensitivity at 1-nm intervals in the range 500–505 nm. At no wavelength was a zero-amplitude trace obtained, as would have been the case were there an isosbestic point. The absorptivity of the intermediate is very close, however, to the absorptivities of the dye and MD at

Table III. Estimates of the Rate Constants of Eq 12 in pH 8.2 HEPPS (25 °C, μ = 0.04 M)

λ, nm	$[Ni]_T$, mM	$[Ni^{2+}]$, mM	$[Ni_4OH_4^{4+}]$, mM	$10^{-4}k_a$, M^{-1} s^{-1}	$10^{-5}k_a'/[Ni_4OH_4^{4+}]$, M^{-1} s^{-1}	k_{-a}, s^{-1}	k_b, s^{-1}	$10^{-4}k_a^{Ni^{2+},D^-}$, M^{-1} s^{-1}
				Dye I				
460	6.0	5.1	0.22	1.18, 1.07	3.2, 2.9	13, 9	28, 28	2.59, 2.35
460	8.0	6.1	0.45	1.04, 0.96	1.8, 1.7	17, 19	29, 21	2.55, 2.38
460	10.0	7.0	0.75	0.96, 1.02	1.3, 1.4	13, 18	20, 25	2.56, 2.73
460	12.0	7.7	1.1	1.05, 0.99	1.1, 1.1	26, 22	29, 25	3.07, 2.89
460	14.0	8.2	1.4	0.93, 0.95	0.9, 1.0	24, 23	25, 25	3.00, 3.06
k_i ± 95% confidence				1.02 ± 0.17				2.72 ± 0.62
560	6.0			0.98		13	24	
560	8.0			0.88		14	20	
560	12.0			0.84		24	23	
k_i ± 95% confidence						18 ± 12	25 ± 7	
				Dye II				
460	6.0			1.73, 1.86	4.7, 5.1	17, 22	30, 37	2.38, 2.56
460	8.0			1.63, 1.93	2.9, 3.4	36, 42	33, 40	2.50, 2.96
460	10.0			1.83, 1.68	2.4, 2.2	49, 44	38, 37	3.06, 2.81
460	12.0			1.78, 1.95	1.9, 2.1	54, 74	42, 43	3.25, 3.56
460	14.0			1.85, 1.74	1.8, 1.7	68, 78	43, 44	3.70, 3.48
k_i ± 95% confidence				1.80 ± 0.24				3.03 ± 1.05
560	6.0			1.62, 1.71		18, 18	34, 40	2.23, 2.35
560	10.0			1.33, 1.29		34, 32	34, 33	2.22, 2.16
560	12.0			1.25, 1.33		44, 57	36, 42	2.28, 2.43
k_i ± 95% confidence				1.42 ± 0.50			38 ± 9	2.28 ± 0.25

wavelengths near where the curves cross.

Rate constants were evaluated via eq 13 and 15–17 from measurements at two wavelengths and several nickel concentrations; the results are collected in Table III. When the parameters of eq 13 were evaluated, the instrument dead time was added to the times measured from the oscilloscope traces after cessation of flow. When this was done, plots of log (absorbance) vs. time extrapolated to the same initial absorbance value for each nickel concentration. The extrapolated values were also the same as the values measured for slower runs at low nickel concentrations. The table also gives the initial equilibrium concentrations of Ni^{2+} and $Ni_4OH_4^{4+}$ present at the various stoichiometric nickel concentrations. Values of k_a determined at 460 nm are fairly precise and independent of nickel concentration, as predicted by eq 12. Values of k_b are less precise but are independent of wavelength and nickel concentration. The computed values of k_{-a} for dye II increase with nickel concentration as a result of small trends in $k_{-a} + k_b$ (eq 15) and k_b/k_{-a} (eq 17) from which the individual values were calculated. A possible trend in the values of k_{-a} for dye I is obscured by the large overall error. A small dependence of the estimated values of k_a on wavelength is indicated for dye II but is not statistically significant at the 95% confidence level.

A wavelength- and concentration-dependent bias in the results can arise from failure of the approximation that $(A - A_\infty)(t)$ is proportional to [D](t) (eq 13). Figure 6 shows the extent to which this approximation fails at the two analytical wavelengths. Since there are differences in absorptivity of the intermediate and the product at both wavelengths, the measured absorbance change is not strictly proportional to [D](t) but contains small contributions from the intermediate. The error from this cause will increase with the initial nickel concentration because of the increase in [X] (eq 14). An alternative explanation for trends in the values of the rate constants is failure of the model, but a severe test of the model is not possible because of the known source of error. If the model is accepted, the most reliable values of the rate constants are obtained at the lowest nickel concentrations.

The rate constants in Table III were estimated at a pH (8.2) where the dyes are not totally dissociated and where the nickel is partially hydrolyzed. Specific rate constants for the interaction of Ni^{2+} with dissociated dye, D^-, were obtained by dividing k_a by $[D^-]/[D]_T$ and $[Ni^{2+}]/[Ni]_T$ and are listed in the last column.

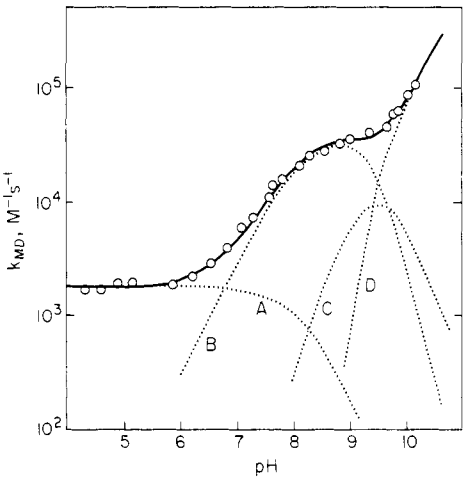

Figure 7. Semilog plot of k_{MD} for dye I as a function of pH. The continuous curve through the data points was calculated by means of eq 24 by summing the contributions shown by the broken curves: A, 1.8 × 10^3 ($f_{Ni^{2+}}f_{DH}$); B, 4.0 × 10^4 ($f_{Ni^{2+}}f_{D^-}$); C, 1.1 × 10^5 ($f_{Ni^{2+}}f_{D^-}\beta_1[OH^-]$); D, 7.9 × 10^5 ($f_{Ni^{2+}}f_{D^-}\beta_3[OH^-]^3$).

Calculations of [X] = $f(t)$ were made via eq 14 by use of the best values of the three empirical rate constants in Table III. The calculations showed that, with 0.1 M nickel ion, 90% of dye I is converted to the intermediate within 4 ms and the change beyond 4 ms is due almost entirely to the conversion of X to MD. An experiment carried out under these conditions confirmed the calculation and gave a direct estimate of k_b for I (21 s^{-1}) in good agreement with the values estimated by fitting data at lower nickel concentrations by eq 13. In addition, measurements made with 0.1 M nickel ion at multiple wavelengths gave an estimate of the absorption curve of X. The first measurable absorbance after mixing should be that of a solution containing ~90% X. The constructed curve of such a solution is shown as the dashed curve in Figure 6. This curve is quite similar in shape to that of MD.

Effect of pH. Measurements made in acetate, MES, HEPPS, and CHES buffers covered the pH range 4–10.3. All runs were made at a constant ionic strength of 0.04 M and

a constant concentration of 0.01 M of the basic component of the buffer. The excess nickel concentration (≤0.4 mM) was such that the pseudo-first-order rate constant was proportional to the nickel concentration. Second-order rate constants for the formation of MD, k_{MD}, were obtained by dividing the initial pseudo-first-order rate constants by the total nickel concentration. Within the indicated range of pH, chelation rates were faster than the nucleation of nickel hydroxide so that no perturbation of the rates from precipitation was seen through 80% reaction.

Figure 7 shows a semilog plot of k_{MD} as a function of pH for dye I. A similar plot was obtained for dye II. The data for the pH range 9–10.3 are considered to deal with acid–base equilibria, which are established on the time scale of the stopped-flow measurements but which represent a metastable condition with respect to precipitation of nickel hydroxide. The profile suggests that various ionic species of dye and nickel are kinetically important over the measured pH range, as described by eq 18–22. The vertical ionization equilibria are

$$DH + Ni^{2+} \longrightarrow H^+ + MD \quad k_{Ni^{2+},DH} \tag{18}$$

$$-H^+ \uparrow\downarrow K_{a2}$$

$$D^- + Ni^{2+} \longrightarrow MD \quad k_{Ni^{2+},D^-} \tag{19}$$

$$-H^+ \uparrow\downarrow$$

$$D^- + NiOH^+ \longrightarrow MD \quad k_{NiOH^+,D^-} \tag{20}$$

$$-H^+ \uparrow\downarrow$$

$$D^- + Ni(OH)_2(aq) \longrightarrow MD \quad k_{Ni(OH)_2,D^-} \tag{21}$$

$$-H^+ \uparrow\downarrow$$

$$D^- + Ni(OH)_3^- \longrightarrow MD \quad k_{Ni(OH)_3^-,D^-} \tag{22}$$

considered to be rapidly established relative to the horizontal chelation reactions. The nickel hydrolysis equilibria are expressed as formation constants

$$\beta_i = \frac{[Ni(OH)_i]}{[Ni^{2+}][OH^-]^i}$$

The log β_i values used in the calculation were taken from Kragten[21] and are, for i = 1–3, respectively, 3.8, 9, and 12. The pyridinium species of the dyes are completely dissociated in the pH range studied.[22,23] All hydrolysis equilibria were considered in calculating concentrations of nickel species, but we found that eq 21 was not needed to describe the pH dependence of the rate constant. The rate expression for the model can be expressed in terms of the Ni^{2+} concentration and β_i and is given by eq 23 where $f_{DH} = [DH]/[D]_T$, $f_{D^-} =$

$$-\text{d ln } [D]_T/dt_{init} = k_{MD}' = [Ni^{2+}](k_{Ni^{2+},DH}f_{DH} + k_{Ni^{2+},D^-}f_{D^-} + k_{NiOH^+,D^-}\beta_1 f_{D^-}[OH^-] + k_{Ni(OH)_3^-,D^-}\beta_3 f_{D^-}[OH^-]^3) \tag{23}$$

$[D^-]/[D]_T = K_{a2}/(K_{a2} + [H^+])$, and $[D]_T = [DH] + [D^-]$. Converting the pseudo-first-order rate constant k_{MD}' to a second-order rate constant gives eq 24 where $f_{Ni^{2+}} =$

$$k_{MD} = k_{MD}'/[Ni]_T = f_{Ni^{2+}}(k_{Ni^{2+},DH}f_{DH} + k_{Ni^{2+},D^-}f_{D^-} + k_{NiOH^+,D^-}\beta_1 f_{D^-}[OH^-] + k_{Ni(OH)_3^-,D^-}\beta_3 f_{D^-}[OH^-]^3 \tag{24}$$

$$[Ni^{2+}]/[Ni]_T = 1/(1 + \beta_1[OH^-] + \beta_2[OH^-]^2 + \beta_3[OH^-]^3).$$

(21) Kragten, J. "Atlas of Metal-Ligand Equilibria in Aqueous Solutions"; Halsted Press: New York, 1978; p 508.
(22) Pease, B. F.; Williams, M. B. *Anal. Chem.* **1959**, *31*, 1044.
(23) Hnilickova, M.; Sommer, L. *Collect. Czech. Chem. Commun.* **1961**, *26*, 2189.

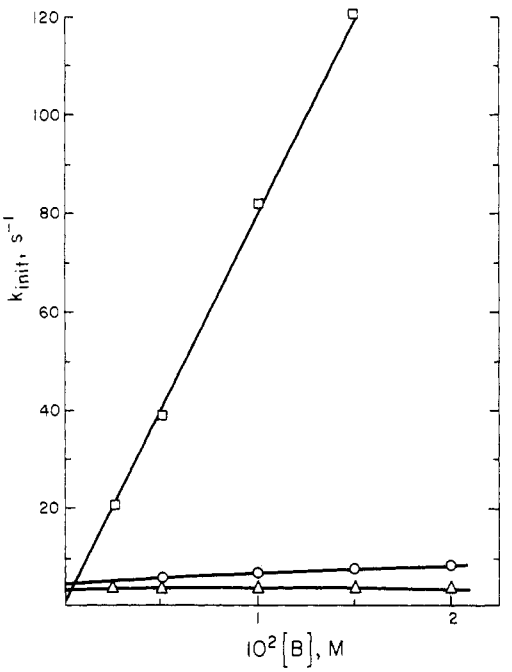

Figure 8. Comparison of the catalytic effect of various amines on the chelation by I at pH 8.0 ([dye] = 2.0×10^5 M; [Ni] = 2.0×10^{-4} M): squares, 2-MeIm, circles, Tris; triangles, TEA.

The continuous curve through the data points of Figure 7 was calculated by summing additive contributions of the terms in eq 24. Similar results were obtained for dye II. At pH 4–5.5, all terms but the first are negligible and $k_{Ni^{2+},DH}$ is evaluated directly from the measured rate constants. At pH 6–8, all terms but the first two are negligible and k_{Ni^{2+},D^-} is evaluated by subtracting the contribution of the first term from the measured k's. All terms but the fourth are negligible at pH 10.3, which permits direct evaluation of $k_{Ni(OH)_3^-,D^-}$. Three nickel species coexist in the pH range 9–10 so that k_{NiOH^+,D^-} had to be evaluated by subtracting the contributions of the second and fourth terms from the measured k's. It is therefore subject to greater error than the other coefficients. The estimated values of the four constants for dye I are $k_{Ni^{2+},DH} = 1.8 \times 10^3$ M^{-1} s^{-1}, $k_{Ni^{2+},D^-} = 4.0 \times 10^4$ M^{-1} s^{-1}, $k_{NiOH^+D^-} = 1.1 \times 10^5$ M^{-1} s^{-1}, and $k_{Ni(OH)_3^-,D^-} = 7.9 \times 10^5$ M^{-1} s^{-1}. The corresponding values for dye II are 2.6×10^3, 4.5×10^4, 1.8×10^5, and 9×10^5 M^{-1} s^{-1}.

Effect of Amine Buffers. Measurements were made at constant pH and ionic strength (0.04 M) as a function of the amine concentration in the buffers over the concentration range of 0.0025–0.02 M. Linear or near-linear plots of k_{init} vs. amine concentration were obtained over a range of pH values. Calculations with the stability constants in Table I showed that several nickel–amine complexes coexisted with Ni^{2+} in the concentration range used. The near-linear kinetic effects indicate that successive replacement of water by amine in the inner coordination sphere produces a nearly additive effect on the reactivity of the nickel(II) complex. The rate constants obtained by extrapolation to zero Tris concentration were the same as those measured in HEPPS buffers.

Figure 8 shows the effect of amine concentration at pH 8.0 on the chelation rates of dye I for several amines. The figure demonstrates the exceptional accelerating effect of complexing with 2-methylimidazole on the rates of chelation by the dyes. Similar results were obtained with imidazole. Although the actual values of the slopes varied a little with pH, the striking effect of the imidazoles remained at all pH values studied.

Effect of Ionic Strength. Measurements were made in a pH 7.9 HEPPS buffer at ionic strengths from 0.001 to 0.08 M. At this pH the only significant contribution to the measured

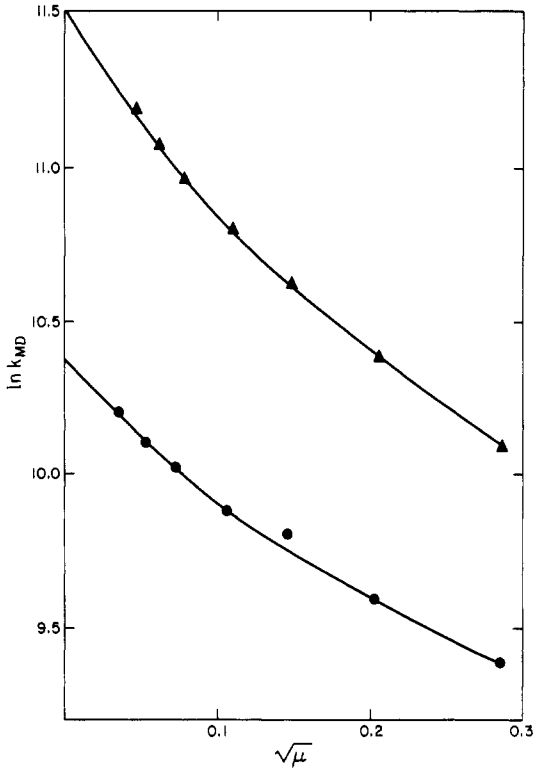

Figure 9. Effect of ionic strength on the chelation of nickel by dye I (circles) and dye II (triangles) in pH 7.9 HEPPS at 25 °C.

rate is from the interaction of dissociated dye with Ni^{2+} (Figure 7). The limiting-law relationship for the rate of a bimolecular reaction of two ions, A and B, as a function of ionic strength μ is given by[24]

$$\ln k = \ln k_0 + 2\alpha Z_A Z_B \mu^{1/2} \quad (25)$$

where k_0 is the second-order rate constant at infinite dilution, Z_A and Z_B are the charges on the ions, and $\alpha = 1.17$ in water at 25 °C. Figure 9 shows plots of ln k_{MD} vs. $\mu^{1/2}$ and shows that eq 25 is valid only at ionic strengths less than about 0.006 M. Values of $Z_A Z_B$ of −2.1 and −3.0 were determined for I and II, respectively, from the initial slopes of the plots. This indicates that the charges on the solubilizing groups of the dyes are sufficiently remote that their influence is small so that I reacts as a monoanion and II reacts as if it had a formal charge of 1.5−.

Discussion

The results are discussed in terms of the mechanism for a multistep chelation (eq 26–29). Here we represent the tridentate dye by L-L-L. A significant finding of this work is that at pH values near 8 the rate-determining step (rds) in this sequence changes with the nickel concentration. At low concentration (0.1–0.4 mM), there is no accumulation of intermediate and the rate of eq 27 is slow and comparable to those of eq 28 and 29. Under these conditions, the steady-state approximation can be applied to intermediates **3** and **4**. Neglecting k_{-3}, we obtain for low nickel concentrations and fixed pH

$$k_{MD} = \frac{K_0 k_1 k_2 k_3}{(k_{-1} + k_2)(k_{-2} + k_3) - k_2 k_{-2}} = K_0 k_1 k_c \quad (30)$$

If we substitute for k_1 the water-exchange rate[25] of 3.0×10^4 s^{-1} for Ni^{2+}, assume a value of 2 M^{-1} for K_0 for dye I reacting as a monoanion,[26] and use the experimental value of 4.0×10^4 M^{-1} s^{-1} for $k_{Ni^{2+}D^-}$ for this dye, we find that $k_c = 0.3$. This coefficient contains the factors giving the probabilities of the intermediates partitioning in the direction of ring closure, and its estimate is only as good as our estimate of K_0. Since the ligand charge is 1− in the D^- species of I and the kinetic effects of ionic strength indicates that the ligand charge is the only one of significance, we feel that our assumed value of K_0 is justified.

If we assume that the biphasic kinetics observed at nickel concentrations near 0.01 M result from the accumulation of an intermediate that lies along the pathway toward MD,[27] then X represents either **3** or **4** and the rates of initial ligation and ring closure are comparable. The manner in which the empirical rate constants in eq 12 are identified with the rate constants in eq 26–29 will depend upon which of the two ring-closure steps is the slower. For reasons given below, we believe that the final step (eq 29) may be the slower. Under this assumption, X ≡ **4** and the steady-state approximation applied to **3**, from which we obtain

$$d[\mathbf{4}]/dt = \frac{K_0 k_1 k_2 [M][L_3]}{k_{-1} + k_2} - \left(k_{-2} - \frac{k_{-2}}{k_{-1} + k_2}\right)[\mathbf{4}] - k_3[\mathbf{4}] \quad (31)$$

From eq 12 we have

$$d[X]/dt = k_a[M][L_3] - k_{-a}[X] - k_b[X] \quad (32)$$

Substituting **4** for X in eq 32 and equating the coefficients in eq 31 and 32 give

$$k_a = \frac{K_0 k_1 k_2}{k_{-1} + k_2} \qquad k_{-a} = k_{-2} - \frac{k_{-2}}{k_{-1} + k_2} \qquad k_b = k_3 \quad (33)$$

With the assumption that the values of K_0 and k_1 for dye I are the same as those that we used above, the value of $k_a^{Ni^{2+},D^-}$ from Table III gives an approximate value of 0.4 for $k_2/(k_{-1} + k_2)$. Thus, the partitioning coefficient for intermediate **3**, k_2/k_{-1}, is near unity. Furthermore, since the values of k_{-a} and k_{-2} cannot differ greatly, we can conclude from the values of k_{-a} and k_b that k_{-2} and k_3 are also of comparable magnitude.

Robinson and White[5] estimated the rate constant for ring closure from the unidentate intermediate of 4-(2-pyridylazo)dimethylaniline (PADA) with nickel(II) and obtained a value of 2.9×10^4 s^{-1}, equal to the water-exchange rate constant for Ni^{2+}, compared to our value of about 25 s^{-1} for I. An absorption curve for Robinson's unidentate intermediate can be estimated from his kinetic data taken at different wavelengths. This has an absorption maximum almost directly between those of the dye and the final bidentate complex. In contrast, the absorption curve of our intermediate closely resembles the curve of the bidentate product from PADA and

(24) Moore, J. W.; Pearson, R. G. "Kinetics and Mechanism"; Wiley: New York, 1981; p 138.

(25) Connick, R. E.; Fiat, D. *J. Chem. Phys.* **1966**, *44*, 4103.
(26) Lin, C.-T.; Bear, J. L. *J. Phys. Chem.* **1971**, *75*, 3705.
(27) Other reaction schemes also give biphasic kinetics.[20]

the tridentate complex from I. This suggests that our intermediate is the bidentate species, **4**. If the first ring closure with the α-PAN dyes (eq 28) is as rapid as that reported by Robinson for PADA, the second ring closure for α-PAN must be the process measured by k_b. The large difference in rates of ring closure with PADA and α-PAN suggests that there may be steric constraints of the final ring closure of α-PAN that are not present in PADA.

In their study of the chelation of nickel(II) by β-PAN, Hubbard and Pacheco[8] concluded that the final ring closure was the rds. They believed that under conditions where the naphthol OH was undissociated the initial bond formation involved the pyridyl nitrogen. Under these conditions, a strong hydrogen bond is formed with an azo nitrogen. They assumed that the hydrogen bond held the naphthol ring in an unfavorable conformation for the final ring closure to take place rapidly. The pK_a's of our α-PAN dyes are low enough to permit measurements at pH values where ionization is complete, and we still find that ring closure is abnormally slow. The existence of the hydrogen bond apparently is not the main reason for the naphthol ring to be in a poor conformation for ring closure.

It has been suggested that the slow ring closure of the intermediate could result from initial ligation with a multinuclear species such as $Ni_4OH_4^{4+}$ instead of with Ni^{2+}.[28] We calculated the concentration of this complex at pH 8.2 for stoichiometric nickel concentrations of 6–14 mM along with the concentrations of Ni^{2+}, $NiOH^+$, $Ni(OH)_2$, $Ni(OH)_3^-$, $Ni(OH)_4^{2-}$, and Ni_2OH^{3+}. Table III shows that kinetically significant concentrations of $Ni_4OH_4^{4+}$ are present in the solutions where biphasic kinetics are observed, although high specific rate constants for the multinuclear complex would be required if chelation occurred exclusively through it in the presence of the much higher concentration of Ni^{2+}. Other evidence against involvement of $Ni_4OH_4^{4+}$ is the fact that the pseudo-first-order rate constant, k_a', is proportional to the concentration of Ni^{2+} but is not proportional to the concentration of $Ni_4OH_4^{4+}$ (column 6, Table III).

The difference in reactivity between the protonated and deprotonated dyes (eq 18 and 19) is relatively small. Most of the effect of protonation can be accounted for by the effect of the charge neutralization on K_0. Changing from an anionic to a neutral ligand is expected to reduce K_0 by a factor of about 10.[29] Very little remaining effect is attributable to a reduction in the rate constant composite of eq 30. This could mean that the oxygen ligand is not involved in the first bond formation.

The increased reactivity of $NiOH^+$ toward D^- relative to that of Ni^{2+} is similar to that found for chelation of nickel(II) by 4-(2-pyridylazo)resorcinol.[6] The high reactivity of $Ni(OH)_3^-$ toward the anionic ligand was unexpected. It is probably the result of labilizing the coordinated water by the hydroxo groups, which more than compensates for the low value of K_0 expected for interaction of reactants of the same charge.

We have shown that the initial chelation products are formed by kinetic rather than thermodynamic control at low nickel concentrations. At pH 8.2 the composite second-order rate constant, k_{MD_2}, must be 5 times greater than k_{MD} to give the initial ratio of complexes. At this pH, $k_{MD} \simeq k_{Ni^{2+},D^-}$ and $k_{MD_2} \simeq k_{NiD^+,D^-}$ where the charges refer to the ligands and the formal charge of the nickel. We will assume that most of the difference between the two composite constants resides in the K_0k_1 products [k_c in k_{MD} (eq 30) is nearly the same as the corresponding composite term in k_{MD_2}]. We anticipate that k_{MD_2} should be smaller than k_{MD} by a factor of about 20 from the statistical factor of 2 and the reduction in K_0 by a factor of about 10 because of the reduced formal charge on nickel in MD. Therefore, k_1 would have to be larger in k_{MD_2} relative to its value in k_{MD} by a factor of about 100 to account for the results. In the absence of experimental exchange rates for water in MD, we can only estimate the additive effect of individual ligands on this rate. Coordination of two pyridine ligands in $Ni(bpy)^{2+}$ increases the water-exchange rate in the complex by a factor of less than 2[30] so that this ligand in MD should produce a very modest increase in k_1. If ligation of the oxygen anion in the dyes produces a similar exchange-rate enhancement as the hydroxide in $NiOH^+$, enhancement by a factor of about 7 is expected.[6] The effect of an azo nitrogen is unknown, but it seems that the large value of k_{MD_2} cannot be accounted for fully by an enhanced water-exchange rate. Following the proposal by Margerum et al., we suggest that part of the large value of k_{MD_2} comes from an exalted value of K_0 for k_{MD_2} whereby the first dye complexed acts as a template for facile addition of a second dye through a stacking interaction of the planar aromatic moieties.[13] The tendency of azo dyes such as these to stack[14] could be enhanced by the presence of the metal cation.

We offer a similar explanation for the unexplained catalytic effect of imidazole and 2-methylimidazole. Coordination of imidazole by Ni^{2+} causes a small reduction in the exchange rate of the remaining water molecules.[31] If imidazole decreases k_1, there seems to be no reason for it to increase k_2 or k_3 (eq 30). It must therefore give an unusually high value of K_0, perhaps by acting as an aromatic template.

Acknowledgment. Helpful discussions of this work with Professor W. P. Jencks, Professor D. W. Margerum, and numerous Kodak colleagues are gratefully acknowledged.

Registry No. I, 10558-11-9; II, 87014-45-7; Ni, 7440-02-0; Im, 288-32-4; 2-MeIm, 693-98-1; Tris, 77-86-1; TEA, 102-71-6; MES, 4432-31-9; HEPPS, 16052-06-5; CHES, 103-47-9.

(28) We are indebeted to Professor D. W. Margerum for this suggestion.
(29) Reference 13, p 13.
(30) Grant, M.; Dodgen, H. W.; Hunt, J. P. *J. Am. Chem. Soc.* **1970**, *92*, 2321.
(31) Hammes, G. G.; Steinfeld, J. I. *J. Am. Chem. Soc.* **1962**, *84*, 4639.